



Research Paper

Numerical investigation on species transport in electroslag remelting dual alloy ingot



Qiang Wang^{a,b,*}, Zhu He^{a,b}, Guangqiang Li^{a,b}, Baokuan Li^c

^aThe State Key Laboratory of Refractories and Metallurgy, Wuhan University of Science and Technology, Wuhan, Hubei 430081, China

^bKey Laboratory for Ferrous Metallurgy and Resources Utilization of Ministry of Education, Wuhan University of Science and Technology, Wuhan, Hubei 430081, China

^cSchool of Metallurgy, Northeastern University, Shenyang, Liaoning 110819, China

HIGHLIGHTS

- First time to study the solute transport in ESR dual alloy ingot.
- The MHD thermosolutal flow in the ESR process was understood.
- The distributions of carbon and nickel in ESR dual alloy were clarified.
- An experiment was carried out to validate the simulation.

ARTICLE INFO

Article history:

Received 14 January 2016

Accepted 17 April 2016

Available online 19 April 2016

Keywords:

Electroslag remelting
Heat transfer
Mass transfer
Solidification
Numerical simulation

ABSTRACT

A transient three-dimensional (3D) comprehensive model has been developed to investigate the solute transport in electroslag remelting (ESR) dual alloy ingot. The solutions of the mass, momentum, energy, and species conservation equations were simultaneously calculated by the finite volume method, and full coupling of the Joule heating and Lorentz force through the solving Maxwell's equations. The movement of the metal droplet was described with the volume of fluid (VOF) approach. Besides, the solidification was modeled by using an enthalpy-based technique, where the mushy zone was treated as a porous medium with an anisotropic permeability. A reasonable agreement between the simulation and the experiment was obtained. The results indicate that the colder metal flowing downward washes the solidification front in the process. The solute-poor metal in the pool displaces the solute-rich metal in the mush region. Meanwhile, the solute enrichment promotes the sinking of the liquid. The inward Lorentz force pushes the metal from the periphery to the bottom. The solutes are deposited at the pool bottom. The negative segregation occurs in the lower part and then rises to positive for the two elements. The maximal positive and negative segregation indexes of the carbon and nickel along the vertical centerline of the ESR dual alloy ingot are 0.38 and -0.19 , and 0.15 and -0.02 , respectively.

© 2016 Elsevier Ltd. All rights reserved.

1. Introduction

Compared with conventional bolted intermediate pressure – low pressure shaft assemblies, the dual alloy single shaft steam turbine offers an obvious increase in power generating efficiency. Such dual alloy shafts are now produced by weld involving long production cycle. ESR is an alternate approach which is able to improve the dual alloy shaft yield and performance. Two different

alloys are connected through welding forming a single electrode, and then the electrode is remelted using ESR furnace. A sound dual alloy ingot therefore is created. Subsequently, the dual alloy ingot is forged and undergoes heat treatments [1]. Macro-segregation is a very common and serious defect in the ingots, which occurs because of the relative movement of the solute-rich or poor liquid and solid phases [2,3]. Especially in the dual alloy ingots, a steep solute concentration gradient is created within the composition transition zone resulting in a poor mechanical property.

Fig. 1 shows a schematic of the ESR process. In this process, an alternating current (AC) is passed from the electrode to the base-plate, creating Joule heating in the highly resistive calcium fluoride-based molten slag. This heating is enough to melt the electrode. The interplay between the self-induced magnetic field and

* Corresponding author at: The State Key Laboratory of Refractories and Metallurgy, Key Laboratory for Ferrous Metallurgy and Resources Utilization of Ministry of Education, Wuhan University of Science and Technology, Wuhan, Hubei 430081, China.

E-mail address: wangqdbdx@163.com (Q. Wang).

Nomenclature

| | | | |
|------------------|--|----------------------|---|
| C_i | mixture mass fraction of species i (wt. pct) | r | radius (m) |
| $C_{i,\ell}$ | mass fraction of species i in liquid phase (wt. pct) | r_e | radius of electrode (m) |
| $C_{i,s}$ | mass fraction of species i in solid phase (wt. pct) | r_m | radius of mold (m) |
| C_0 | nominal concentration (wt. pct) | t | time (s) |
| $C_{p,m}$ | specific heat of metal at constant pressure (J/(kg K)) | T | temperature (K) |
| $C_{p,s}$ | specific heat of slag at constant pressure (J/(kg K)) | T_ℓ | liquidus temperature (K) |
| d_1 | primary dendrite arm spacing (μm) | T_{pure} | melting point of the pure iron (K) |
| d_2 | secondary dendrite arm spacing (μm) | T_s | solidus temperature (K) |
| $D_{i,\ell}$ | diffusion coefficient of species i in the liquid (m^2/s) | ΔT | superheat degree of the metal at the inlet (K) |
| E | internal energy of mixture phase (J/ m^3) | \mathbf{v} | velocity (m/s) |
| f_ℓ | liquid fraction | x, y, z | Cartesian coordinates |
| \mathbf{F}_e | Lorentz force (N/m^3) | <i>Greek symbols</i> | |
| \mathbf{F}_d | turbulent damping force (N/m^3) | α | volume fraction of metal |
| \mathbf{F}_s | solute buoyancy force (N/m^3) | $\bar{\eta}$ | magnetic diffusivity of mixture phase ($\Omega \text{ m}^2/\text{H}$) |
| \mathbf{F}_t | thermal buoyancy force (N/m^3) | $\bar{\mu}$ | dynamic viscosity of mixture phase (Pa s) |
| G' | thermal gradient (K/m) | μ_t | turbulent viscosity (Pa s) |
| \mathbf{H} | magnetic field intensity (A/m) | μ_0 | vacuum permeability (H/m) |
| \hat{H} | complex amplitude (A/m) | $\bar{\rho}$ | density of mixture phase (kg/m^3) |
| I_0 | root mean square of the current (A) | ρ_m | density of metal (kg/m^3) |
| \mathbf{J} | current density (A/m^2) | ρ_s | density of slag (kg/m^3) |
| k_i | partition coefficient of species i | ξ | coefficient in Eq. (21) which represents the power efficiency |
| k_{eff} | effective thermal conductivity ($\text{W}/(\text{m K})$) | $\bar{\sigma}$ | electrical conductivity of mixture phase ($\Omega^{-1} \text{ m}^{-1}$) |
| K_1 | permeability component parallel to the isotherm (μm) | ω | angular frequency (Hz) |
| K_2 | permeability component perpendicular to the isotherm (μm) | ϕ | mixture phase property |
| L | latent heat of fusion (J/kg) | ϕ_m | metal property |
| \dot{m} | melt rate (kg/s) | ϕ_s | slag property |
| m_i | liquidus slope of species i (K/wt. pct) | | |
| p | pressure (Pa) | | |
| Q_j | Joule heating (W/m^3) | | |

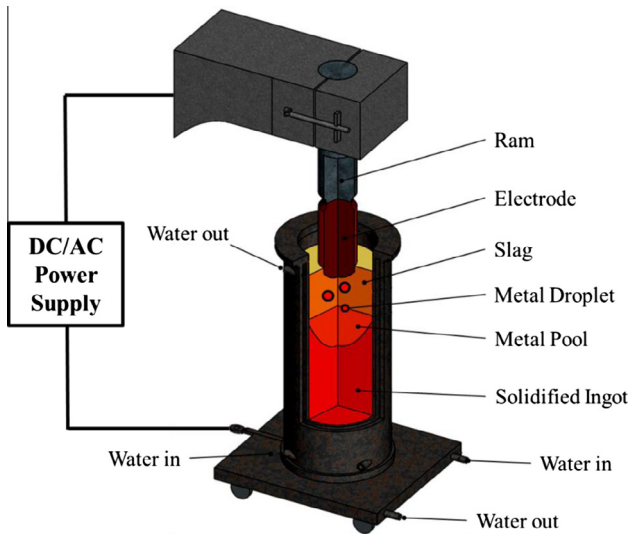


Fig. 1. Schematic of electroslag remelting process.

the AC products Lorentz force. Dense metal droplets sink through the less dense molten slag to form a liquid metal pool in the water-cooled mold. The metal is solidified as it loses heat to the mold, forming an ingot. A liquid metal pool is maintained throughout the process. Finally, the AC is gradually reduced until all of the metal freezes [4,5].

Given the complicated phenomena involved, and the difficulty and expense of performing experiments on a real apparatus,

numerical simulations present an attractive method to understanding the solute distribution in various ingots. The species transportation models of heavy ingots have been well established [6–13]. Melt convection and macrosegregation in a large steel ingot were simulated by Gu et al. [14]. The fully coupled governing conservation equations for the mass, momentum, energy, and species in the liquid, mush, and solid were solved by the finite volume method. Moreover, the heat transfer in the mold and insulation materials, as well as the formation of a shrinkage cavity at the top, was also taken into account. The predicted macrosegregation along the vertical centerline was generally in good agreement with the measurements except at the ingot bottom. The neglect of the sedimentation of free equiaxed crystals was supposed to be responsible for the difference. A similar work has been done by Li et al. [15]. The main feature of their work was the consideration of the columnar-to-equiaxed transition and the crystal sedimentation. The results indicated that the equiaxed sedimentation was an important mechanism responsible for the formation of negative segregation, because it significantly influenced the flow pattern in the lower part of the heavy ingots. The solidification shrinkage however was ignored in their work. An experimental investigation on the channel segregation in the large ingot has been conducted by Li et al. [16]. The movement of the oxide-based inclusion during the steel freezing was particularly studied. A competition between the newly discovered inclusion flotation and the traditionally recognized thermosolutal flow was found, and the channel segregation would occur when the inclusion sufficient volume fraction-driven flotation becomes stronger than the thermosolutal flow.

With forced cooling and Lorentz force, the species transport in ESR ingots remarkably changes [17]. The macrosegregation occurred in the mushy zone during the ESR process has been

Download English Version:

<https://daneshyari.com/en/article/7047718>

Download Persian Version:

<https://daneshyari.com/article/7047718>

[Daneshyari.com](https://daneshyari.com)